



## LJMU Research Online

**Bhullar, KA, Horgan, MIM, Le, A, Fania, D, Wuhrer, R, Razmovski-Naumovski, V, Chan, K, Castignolles, P and Gaborieau, M**

**Assessing the quantification of acetylation in konjac glucomannan via ATR-FTIR and solid-state NMR spectroscopy**

**<https://researchonline.ljmu.ac.uk/id/eprint/17381/>**

### Article

**Citation** (please note it is advisable to refer to the publisher's version if you intend to cite from this work)

**Bhullar, KA, Horgan, MIM, Le, A, Fania, D, Wuhrer, R, Razmovski-Naumovski, V, Chan, K ORCID logoORCID: <https://orcid.org/0000-0002-2948-8324>, Castignolles, P and Gaborieau, M (2022) Assessing the quantification of acetvlation in koniac glucomannan via ATR-FTIR and**

LJMU has developed **LJMU Research Online** for users to access the research output of the University more effectively. Copyright © and Moral Rights for the papers on this site are retained by the individual authors and/or other copyright owners. Users may download and/or print one copy of any article(s) in LJMU Research Online to facilitate their private study or for non-commercial research. You may not engage in further distribution of the material or use it for any profit-making activities or any commercial gain.

The version presented here may differ from the published version or from the version of the record. Please see the repository URL above for details on accessing the published version and note that access may require a subscription.

For more information please contact [researchonline@ljmu.ac.uk](mailto:researchonline@ljmu.ac.uk)

<http://researchonline.ljmu.ac.uk/>



## Assessing the quantification of acetylation in konjac glucomannan via ATR-FTIR and solid-state NMR spectroscopy

Kash A. Bhullar<sup>a</sup>, Michael I.M. Horgan<sup>a</sup>, Ashley Le<sup>a</sup>, David Fania<sup>b</sup>, Richard Wuhrer<sup>b</sup>,  
Valentina Razmovski-Naumovski<sup>c,d</sup>, Kelvin Chan<sup>c,e</sup>, Patrice Castignolles<sup>a,f,1,\*</sup>,  
Marianne Gaborieau<sup>a,1,\*</sup>

<sup>a</sup> Western Sydney University, Australian Centre for Research on Separation Science (ACROSS), School of Science, Parramatta Campus, Locked Bag 1797, Penrith, NSW 2751, Australia

<sup>b</sup> Western Sydney University, Advanced Materials Characterisation Facility, Parramatta Campus, Locked Bag 1797, Penrith, NSW 2751, Australia

<sup>c</sup> Western Sydney University, NICM Health Research Institute, School of Science, Campbelltown Campus, Locked Bag 1797, Penrith, NSW 2751, Australia

<sup>d</sup> South West Sydney Clinical Campuses, Discipline of Medicine, University of New South Wales Sydney, NSW 2170, Australia

<sup>e</sup> Liverpool John Moores University, School of Pharmacy & Biomolecular Sciences, Liverpool L3 3AF, United Kingdom

<sup>f</sup> Sorbonne University, Parisian Institute of Molecular Chemistry, UMR 8232, Polymer Chemistry team, 75252 Paris, France

### ARTICLE INFO

#### Keywords:

Konjac glucomannan  
Degree of acetylation  
Quantification  
Solubility  
Solid-state NMR spectroscopy  
ATR-FTIR spectroscopy

### ABSTRACT

Dietary fiber like konjac glucomannan (KGM) is important in maintaining good human health. There is no established method for quantifying the average degree of acetylation *DA* of this polysaccharide. Polysaccharides are notoriously difficult to dissolve. In this study, KGM could not be fully dissolved in common solvents and was characterized in the solid state. ATR-FTIR spectroscopy enabled a fast qualitative assessment of acetylation, selective to the outer layer of KGM particles, and identifying excipients like magnesium stearate. Average *DA* was quantified for the first time with solid-state <sup>13</sup>C NMR in KGM: semi-quantitative measurements on the same arbitrary scale by cross polarization (1 to 2 days) were calibrated with a few longer single-pulse excitation measurements (approximately 1 week). *DA* values ranged from 4 to 8% of the hexoses in the backbone, in agreement with previously reported values. This method could be used for quality control and standardization of KGM products.

### 1. Introduction

Glucomannan is a neutral polysaccharide abundant in plant bulbs, tubers or softwoods (Alonso-Sande, Teijeiro-Osorio, Remunan-Lopez, & Alonso, 2009; Gidley, McArthur, & Underwood, 1991). The most commonly used and studied glucomannan is konjac glucomannan (KGM) (Chua, Baldwin, Hocking, & Chan, 2010; Rinaudo, 2006). It is extracted from the root of *Amorphophallus konjac* K. Koch (Araceae), a tuber plant native to Southeast and East Asia (Chua et al., 2010). There, it has been used as a food source and as a traditional medicine (Chua et al., 2010). KGM is increasingly researched for its desirable properties: it is inexpensive, biodegradable, biocompatible, and able to form films and gels

(Gomes Neto et al., 2019; Wu et al., 2012). KGM and its derivatives have many applications in the pharmaceutical industry as an excipient (Alonso-Sande et al., 2009), in the food industry as a texture modifier and thickener (Kok, Abdelhameed, Ang, Morris, & Harding, 2009), in water purification (Zhu, 2018), in food packaging and cosmetics (Zhang, Xie, & Gan, 2005), and potentially in drug delivery (Alonso-Sande et al., 2009). KGM is a dietary fiber and has no calorific content; it is thus used as a satiety agent and as an ingredient in low-calorie foods (Chua et al., 2010; Singh, Singh, & Arya, 2018) and can potentially treat obesity-related disorders (Chua et al., 2010; Keithley & Swanson, 2005). However, its incomplete characterization at the molecular level affects the quality control of the products.

**Abbreviations:** ATR-FTIR, attenuation total reflectance Fourier-transform infrared; CP, cross polarization; *DA*, degree of acetylation; DMAc, *N,N*-dimethyl acetamide; DMSO, dimethyl sulfoxide; KGM, Konjac glucomannan; MAS, magic-angle spinning; NMR, nuclear magnetic resonance spectroscopy; RSD, relative standard deviation; SEC, size-exclusion chromatography; SNR, signal-to-noise ratio (of signal A in <sup>13</sup>C NMR spectra); SPE, single-pulse excitation

\* Corresponding authors at: Western Sydney University, Australian Centre for Research on Separation Science (ACROSS), School of Science, Parramatta Campus, Locked Bag 1797, Penrith, NSW 2751, Australia.

E-mail addresses: [patrice.castignolles@sorbonne-universite.fr](mailto:patrice.castignolles@sorbonne-universite.fr) (P. Castignolles), [m.gaborieau@westernsydney.edu.au](mailto:m.gaborieau@westernsydney.edu.au) (M. Gaborieau).

<sup>1</sup> Members of the European Polysaccharide Network of Excellence (EPNOE).

<https://doi.org/10.1016/j.carbpol.2022.119659>

Received 6 March 2022; Received in revised form 11 May 2022; Accepted 23 May 2022  
0144-8617/© 20XX

The structure proposed (Fig. 1) is a hetero-polysaccharide composed of  $\beta(1,4)$  linked D-glucose and D-mannose, with branching and acetylation (Alonso-Sande et al., 2009; Kato & Matsuda, 1969; Kok et al., 2009). Mannose-to-glucose ratios are reported at about 1.6. Branching with short side chains is reported to occur at the C-3 position of some hexoses or at the C-6 position of some glucose residues. Acetylation is reported to occur at the C-6 position of 5 to 10% of the hexoses. The weight-average molar mass of KGM reported from size-exclusion chromatography (SEC) coupled to multi-angle light scattering detection is typically  $10^4$  to  $2 \times 10^6$  g.mol<sup>-1</sup> (Alonso-Sande et al., 2009; Kok et al., 2009; Ratcliffe, Williams, Viebke, & Meadows, 2005). Branching and the presence of different monomer units (different hexoses) may affect the separation by SEC and thus, the determined molar masses (Gaborieau & Castignolles, 2011).

Complete molecular dissolution is required for a successful separation and meaningful characterization of molecules in solution, with techniques like chromatography, SEC or nuclear magnetic resonance spectroscopy (NMR). It is also required for a homogeneous chemical modification. Complete dissolution is usually assumed when a clear, transparent solution is obtained but this is not sufficient to prove complete dissolution as aggregates (i.e., microgels) may be present (Maniego, Sutton, Gaborieau, & Castignolles, 2017; Schmitz, Dona, Castignolles, Gilbert, & Gaborieau, 2009; Thevarajah, Bulanadi, Wagner, Gaborieau & Castignolles, 2016a). Polysaccharides are notoriously difficult to dissolve (Rebierre et al., 2016; Schmitz et al., 2009; Thevarajah et al., 2016a). KGM's numerous hydrogen bonds make its dissolution difficult in aqueous (Alonso-Sande et al., 2009) and organic solvents (El Seoud, Koschella, Fidale, Dorn, & Heinze, 2007; Ratcliffe et al., 2005). Water is a poor solvent for konjac glucomannan (Kruk, Kaczmarczyk, Ptaszek, Goik, & Ptaszek, 2017). Homogeneous KGM dispersions have been reported using sonication or microwave irradiation; however, this causes degradation (Ratcliffe et al., 2005). Studies reporting homogeneous dispersions using water, aqueous cadoxen (CdO/ethylenediamine) (Nishinari, 2000) and NaOH/thiourea (Yang, Xiong, & Zhang, 2002), have not confirmed KGM's complete dissolution.

Since the 1920s, the complex KGM structure has been investigated using different methods (Katsuraya et al., 2003; Kok et al., 2009; Nishinari, Williams, & Phillips, 1992) with the 1980s introducing solution-state NMR (Brigden & Wilkinson, 1985). <sup>1</sup>H solution-state NMR measurements showed acetyl groups on mannose and glucose units (Williams et al., 2000). However, it is rarely mentioned whether the NMR spectra presented are quantitative or if the samples were fully soluble. Thus, solid-state methods (e.g., spectroscopy) should be used for a

reliable analysis of the whole sample. Solid-state NMR can characterize polymers at the molecular level in terms of average composition, packing and chain dynamics (Spiess, 2017). Chain conformations and impurities (lipids, proteins) in 'dry', hydrated powders and gels of KGM were analyzed by solid-state <sup>13</sup>C NMR (Felix da Silva et al., 2020; Gidley et al., 1991). Solid-state <sup>13</sup>C NMR of KGM exhibits sufficient resolution for identifying acetylation (Felix da Silva et al., 2020); however, insufficient information was provided to judge whether the spectra were quantitative.

Attenuation total reflectance Fourier transform infrared (ATR-FTIR) spectroscopy is cheaper and faster than solid-state NMR. KGM was qualitatively analyzed by ATR-FTIR spectroscopy, with bands in the 1800–800 cm<sup>-1</sup> region originating from glucose, mannose units and acetyl groups (Felix da Silva et al., 2020); however, quantification has been limited, due to signal overlap and difficulty in obtaining quantitative data.

Variability in KGM's composition, structure and size has been reported between studies depending on analytical procedures (Alonso-Sande et al., 2009). Acetylation is a relevant property to measure as it affects KGM's solubility in water, the viscosity of its dispersions, and its gelation behavior (Alonso-Sande et al., 2009; Du, Li, Chen, & Li, 2012; Kok et al., 2009; Williams et al., 2000). Therefore, the aim of the study is to quantify the average degree of acetylation DA in KGM. The research questions addressed in the present work are: (a) whether konjac glucomannan is soluble in common solvents, and (b) whether ATR-FTIR and solid-state NMR spectroscopy can quantify acetylation in KGM if solubility is incomplete.

## 2. Material and methods

### 2.1. Materials

Milli-Q quality water (Millipore, Bedford, MA, USA) was used. Sodium hydroxide pellets (98%, NaOH), dimethyl sulfoxide ( $\geq 99.5\%$ , DMSO), lithium bromide (99%, LiBr), sodium chloride (99.5%, NaCl), *N,N*-dimethyl acetamide ( $\geq 99.5\%$ , DMAc), acetic anhydride (99%), ethanol (99%), and adamantane (99%) were from Sigma-Aldrich. Singly <sup>13</sup>C-labelled alanines (1-<sup>13</sup>C, 2-<sup>13</sup>C, or 3-<sup>13</sup>C; 99%) were from Cambridge Isotope laboratories, Inc. Anhydrous DMSO was produced using molecular sieves (208,582, 3 Å, 8–12 mesh beads from Sigma-Aldrich). Soluble starch powder was from Fisons (Homebush, NSW, Australia). Glucose powder (Dextrose, bacteriological grade) was from Oxid Ltd., London. KGM samples are described in Table 1.

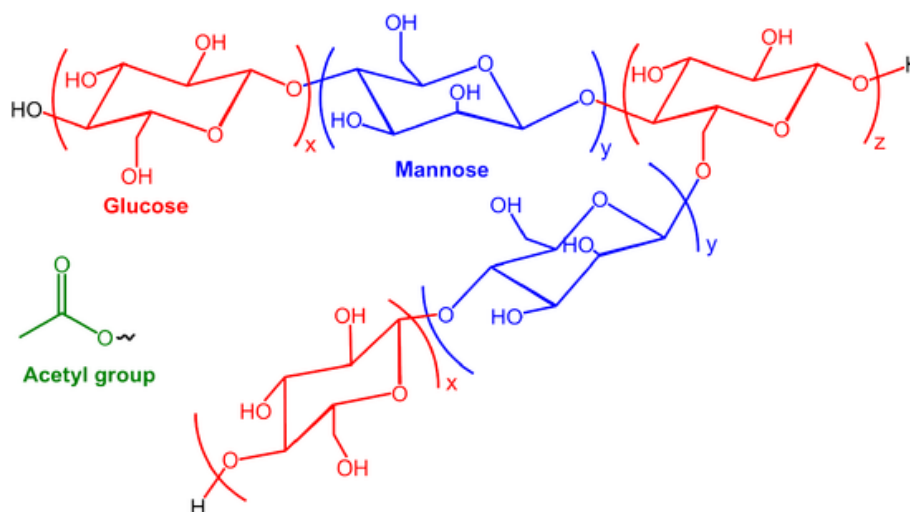


Fig. 1. Schematic representation of KGM structure composed of glucose (red) and mannose (blue) units with acetylation and branching. The acetyl group (green) was reported to be at the C-6 position on some of the hexoses (CH<sub>2</sub>-O-H becoming CH<sub>2</sub>-O-acetyl). (For interpretation of the references to colour in this figure legend, the reader is referred to the web version of this article.)

**Table 1**  
KGM samples used in the study.

Sample	Description	Product name, supplier	Batch number	Composition (as listed by supplier)
KGMA	Powder*	Konjac Glucomannan Excel Slim Fiber M&S Colloid Technology Ltd., Hong Kong, China	T-4255	KGM 100%
KGMB	Powder#	100% Pure Glucomannan Powder, NOW Foods Ltd., Bloomingdale, Illinois, USA	6513 V2	KGM 100%
KGMC	Powder#	Fiber dense Glucomannan, Swanson Health Products, Inc., Fargo, ND, USA	SW1163	KGM, gelatin, rice flour, microcrystalline cellulose, magnesium stearate, silica
KGMD	Powder#	Double Strength Glucomannan, Puritan's Pride, INC. Holbrook, NY, USA	B36120 01B	KGM, gelatin, vegetable magnesium stearate
KGME	Powder*	Luralean® Glucomannan Powder (Grade A), AHD International, Atlanta, Georgia, USA	GC121231A	KGM 100%
KGMF	Powder*	Glucomannan Luralean® medium, Nutra Novus, Atlanta, Georgia, USA	121224RS	KGM 100%
KGMG	Powder*	Arkocaps Konjac, Arkopharma laboratories pharmaceutiques, Carros, France	CCP1489A	KGM, hydroxypropyl methylcellulose, magnesium stearate
KGMS <sup>∞</sup>	Wet, long, pasta-like*	Slendier Slimpasta Spaghetti, D'Lite FoodPacific Pty Ltd., Mt. Waverley, Victoria, Australia	2013	KGM, starch, gelatin

\* from corm, # from root.

<sup>∞</sup> not included in acetylation assessment since only available as gel-like pasta (not solid).

## 2.2. Methods

### 2.2.1. Dissolution tests

Samples (starch, glucose, KGM except KGMG) were prepared at nominal concentrations of 0.625 g.L<sup>-1</sup>, 0.5 g.L<sup>-1</sup> and/or 0.1 g.L<sup>-1</sup> in different solvents: aqueous (water, water with 5% NaCl, with 98% NaCl, with 0.01 M NaOH or with 0.1 M NaOH) and organic (DMSO, DMSO with 98% LiBr, anhydrous DMSO, anhydrous DMSO with 5% LiBr, anhydrous DMSO with 98% LiBr, DMAc, DMAc with 5% LiBr), where percentages are weight/weight (w/w). All samples were prepared in 2 mL flat-bottom glass vials, heated at 80 °C for 3 h in a water bath, and briefly taken out for visual observation every hour (more details in supplementary material).

### 2.2.2. KGM acetylation

KGMB acetylation into KGMB-ac followed a published method (Koroskenyi & McCarthy, 2001). Briefly, KGMB powder (1.0 g), acetic anhydride (10 mL) and sodium hydroxide aqueous solution (50% (w/w)) were stirred in a round-bottom flask (50 mL) for 3 h at room temperature under reflux. The sample was vacuum filtered, washed with ethanol and freeze-dried.

### 2.2.3. FTIR spectroscopy

The FTIR spectra of powder samples were recorded with a 2 cm<sup>-1</sup> resolution and 64 scans using a Bruker Vertex 70 spectrometer with a diamond ATR window crystal; the data treated and normalized using the Bruker OPUS software suite (unless specified). A background was

measured before each measurement. For quantification, 10 replicate ATR-FTIR spectra were collected for each sample; spectra were treated with ATR correction, smoothing over 25 points, and baseline correction with 51 iterations. The precision was assessed through the standard deviation of the 10 DA values determined from the replicate spectra for each sample.

### 2.2.4. Solid-state NMR spectroscopy

Solid-state <sup>1</sup>H and <sup>13</sup>C NMR spectra were recorded on a Bruker DPX200 spectrometer operating at Larmor frequencies of 200 MHz and 50 MHz for <sup>1</sup>H and <sup>13</sup>C, respectively. A commercial double-resonance, magic-angle spinning (MAS) probe was used. Samples were spun at the magic angle at 10 kHz (for single pulse excitation, SPE) and 12 kHz (for cross polarization, CP) in rotors with a 4-mm outer and a 3-mm inner diameter. For <sup>1</sup>H and <sup>13</sup>C SPE-MAS experiments, the 90° pulse was optimized using adamantane; for <sup>13</sup>C CP-MAS experiments power levels were optimized using a mixture of three <sup>13</sup>C singly labelled alanine. The <sup>1</sup>H and <sup>13</sup>C chemical shifts scales were externally referenced to the CH resonance of adamantane at 1.64 and 38.48 ppm, respectively (Morcombe & Zilm, 2003).

<sup>1</sup>H NMR spectra were recorded using a 5 μs 90° pulse length, a 3 s repetition delay and at least 32 scans. <sup>13</sup>C CP-MAS NMR spectra of KGMA were recorded with 0.2, 0.5, 1 and 2 ms contact times, with a 5 s repetition delay and 8192 scans, then recorded with 3, 4, 5, 5.5, 6, and 7 ms contact times, with a 5 s repetition delay and 32,768 scans. <sup>13</sup>C CP-MAS NMR experiments of KGMB, KGMB-ac, KGMC, KGMD, KGME, KGMF and KGMG were recorded with a 5.5 ms contact time, a 5 s relaxation delay and 32,769 scans. Quantitative <sup>13</sup>C SPE-MAS spectra were recorded for KGMA, KGMB, KGMB-ac and KGME with a 100 s repetition delay (at least five times longer than T<sub>1</sub> for signals A to D), using 90° pulse lengths of 3.75, 4.25, 4.25 and 4.15 μs, respectively, with 4096, 3111, 7534 and 4427 scans, respectively. The signal-to-noise ratio (SNR) was determined with the 'sino cal' function of Bruker Topspin 3.2, with signal in the range of 15–30 ppm, and noise over the range of 200–340 ppm with a 40-ppm range.

## 3. Results & discussion

Original data of this study (FTIR and NMR data) are available at Mendeley Data (<http://dx.doi.org/10.17632/y26t6t7wvz.2>).

### 3.1. Visual observation of dissolution

To date, no complete molecular dissolution of native KGM has been reported. In this study, visual observation revealed incomplete dissolution of KGM in aqueous media after 3 h at 80 °C while (visually) complete dissolution occurred for glucose and soluble starch in the same conditions (Table S3 in supplementary material). KGM strongly interacts with water through its numerous hydroxy groups. Acetyl groups replace hydroxy groups on KGM, making the polysaccharide more hydrophobic and thus, could be expected to make it less water-soluble. However, acetylation is reported to increase KGM's water-solubility (Alonso-Sande et al., 2009; Stephen & Churms, 2006). In this study, KGM concentration in water was decreased from 0.625 to 0.5 then to 0.1 g.L<sup>-1</sup> to promote KGM solvation by decreasing the proximity of KGM chains in solution. KGM dispersions in water exhibited aggregates visible as particles at higher concentrations, while smaller aggregates resulted in turbidity of the dispersion at lower concentrations. Salt (NaCl) was added to water to promote the disruption of the hydrogen bonds which are preventing KGM dissolution, following an approach that was successful with starch (Schmitz et al., 2009). NaCl had no visible effect on KGM solubility at lower salt concentration (5%) and a negative effect at higher salt concentration (98%) with some samples exhibiting an increase in the size of the particles visible in the dispersion. pH was then increased to promote the disruption of the hydrogen

bonds. At higher KGM and lower NaOH concentration (0.01 M), KGM solubility slightly improved, with no changes observed at lower KGM and higher NaOH concentration (0.1 M). NaOH addition has been reported to promote KGM dissolution but also its deacetylation, leading to KGM gelation (Huang, Takahashi, Kobayashi, Kawase, & Nishinari, 2002). Aqueous solvents tested in this study were unable to completely dissolve KGM, thus organic solvents commonly used for polysaccharide dissolution were tested.

KGM dissolution was visually incomplete in organic media after 3 h at 80 °C, while dissolution was (visually) complete for glucose and soluble starch in some of these conditions (Table S4). This was unexpected for KGM, as similar complex polysaccharides, like starch, have dissolved in DMSO-based solvents (Schmitz et al., 2009). Adding LiBr as a hydrogen bond disruptor to DMSO did not visually improve KGM dissolution; neither did using DMAc (without or with LiBr), another solvent commonly used for cellulose dissolution (Furuhata, Koganei, Chang, Aoki, & Sakamoto, 1992).

Thus, KGM was not fully soluble in the solvents tested (aqueous or organic). At best, very fine dispersions were formed. A meaningful characterization of KGM in solution was therefore not possible. Methods that characterize solid-state samples were thus chosen for assessing acetylation.

### 3.2. ATR-FTIR spectroscopy

The acetyl group is observed in FTIR spectra of KGM through the characteristic band of its stretching vibration  $\nu(\text{C}=\text{O})$  at 1730  $\text{cm}^{-1}$  (Chua et al., 2012) (see Table S5 for complete signal assignment). FTIR data acquisition and treatment were first examined with the intensity and resolution of this band in mind (Figs. S2 to S5). Although transmission FTIR overcame the limited penetration depth of the irradiation in the sample (about 2  $\mu\text{m}$  (Sevenou, Hill, Farhat, & Mitchell, 2002) in ATR-FTIR), it provided insufficient resolution for the signal at 1730  $\text{cm}^{-1}$  (Fig. S3 and S4). For quantification, ATR-FTIR data was analyzed with ATR correction, smoothing over 25 points, and baseline correction with 51 iterations (Fig. 2).

The FTIR bands most relevant to KGM's acetylation are from carbonyl stretching at 1730  $\text{cm}^{-1}$ , water molecule in-plane deformation at 1655  $\text{cm}^{-1}$ , and ether stretching at 1015  $\text{cm}^{-1}$  (labelled D, E and P in Fig. 2; see Table S5 for complete signal assignment). The FTIR region of 4000 to 1800  $\text{cm}^{-1}$  is similar for all KGM samples, except for sharp bands (B and C) at 2850 and 2920  $\text{cm}^{-1}$  showing the presence of magnesium stearate excipient in KGMC, KGMD and KGMG (in larger proportion in KGMG than KGMC or KGMD). The other bands of this excipient at ~3300, 1580, 1465 and 750  $\text{cm}^{-1}$  (Table S5), are not expected to interfere with FTIR acetylation studies.

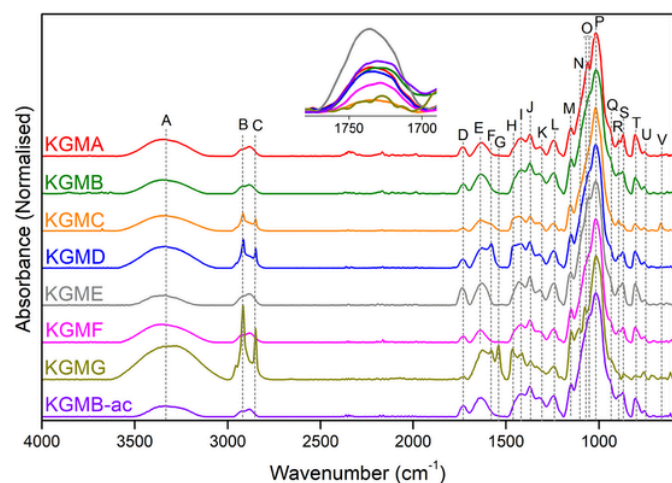


Fig. 2. ATR-FTIR spectra of KGM samples (see Table S5 for signal assignment).

Ten replicate ATR-FTIR spectra were recorded from 1800 to 600  $\text{cm}^{-1}$  for each KGM sample (Figs. S6 to S13) and were highly repeatable. Quantifying DA in KGM requires (1) resolving one band belonging to the acetyl group and one belonging to each hexose as a reference, and (2) extracting the relative ratio of the corresponding functional groups in the sample from their relative intensities. The acetyl band at 1730  $\text{cm}^{-1}$  was resolved (Fig. 2); however, no hexose bands were fully resolved. It was decided to put all ATR-FTIR spectra on the same “hexose scale” by normalizing them to the same intensity (height) of the most intense band (P) of hexose rings at 1015  $\text{cm}^{-1}$ . DA was then estimated as  $DA_{\text{IR}}$  (in arbitrary units a.u.) as the area of the acetyl band D on that arbitrary scale. The precision was assessed from the 10 values determined from replicate spectra for each sample.

$DA_{\text{IR}}$  values for KGM samples (except KGMB-ac) ranged from 1.7 to 10.7 a.u. (see Table S8 for values). These are not absolute (quantitative) values: firstly, because the acetyl band areas were normalized with a band height, not a band area, for the hexoses, and secondly, band intensities in FTIR spectroscopy are not directly proportional to the concentration of the corresponding functional groups in the sample. These also depend on extinction coefficients, which were not considered here and may not be known. Nevertheless, qualitative comparisons between samples are possible with this measurement. For example, it was estimated that the acetylation reaction carried out on KGMB to yield KGMB-ac significantly increased its DA by 50 to 110%. The limitations of ATR-FTIR spectroscopy to quantify DA in KGM are addressed via the use of solid-state NMR, which presents the advantage of measuring the whole sample.

### 3.3. Solid-state NMR spectroscopy

#### 3.3.1. $^1\text{H}$ vs $^{13}\text{C}$ NMR

Although solid-state  $^1\text{H}$  NMR is faster (typically minutes) than solid-state  $^{13}\text{C}$  NMR (typically hours to days), the method usually exhibits a lower resolution. Solid-state  $^1\text{H}$  NMR spectra of KGM samples exhibited a broad signal around 3 to 5 ppm (Fig. 3a). KGME and KGMG exhibited a broader signal than other samples, indicating a lower mobility of the polymer chains. One narrow, low intensity signal (at 1.1 ppm) was observed for KGMG. This may originate in very mobile molecules which could be low amounts of magnesium stearate excipient (methylene moieties of stearate exhibit their most intense  $^1\text{H}$  NMR signal at a chemical shift of 1.25 ppm according to a simulation with ChemDraw, CambridgeSoft). Solid-state  $^1\text{H}$  NMR resolution was insufficient to selectively observe acetyl group signals and thus to investigate acetylation in KGM.

Solid-state  $^{13}\text{C}$  NMR improved the spectral resolution for KGM (Fig. 3b). The  $^{13}\text{C}$  SPE-MAS NMR spectrum of KGMB-ac was consistent with published spectra recorded in similar conditions (Gidley et al., 1991; Vieira & Gil, 2005). Signals were resolved for the acetyl group: a methyl signal at 21 ppm and a carbonyl signal at 173 ppm (labelled A and E, respectively, in Fig. 3b; see Table S6 for complete signal assignment). The signal at 103 ppm (D in Fig. 3b) corresponds to one carbon in each of the hexoses. The DA can thus, in principle, be quantified in KGM by  $^{13}\text{C}$  NMR via integration of signals D and either A or E. However, the limited sensitivity of signals A and E renders quantification difficult as the acquisition of a quantitative spectrum with good sensitivity would require long measuring times (approximately 1 week for each sample).

#### 3.3.2. Semi-quantitative $^{13}\text{C}$ CP-MAS

$^{13}\text{C}$  CP-MAS NMR enabled the measurement of the methyl and carbonyl signals from the acetyl group in a significantly shorter duration (1 to 2 days, Fig. 4b) and provided semi-quantitative data (Gaborieau, Nebhani, Graf, Barner, & Barner-Kowollik, 2010). Here, semi-quantitative refers to quantifying a ratio of signal intensities with a consistent systematic error so that the ratio is determined on the same arbitrary scale for all samples. This allows comparisons between samples,

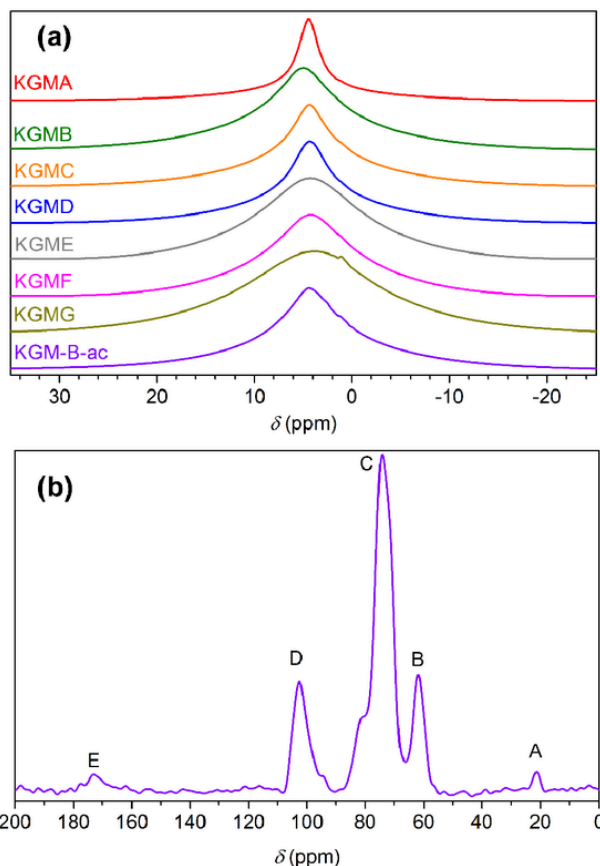


**Fig. 3.** (a) Solid-state  $^1\text{H}$  MAS NMR spectra of all KGM samples and (b)  $^{13}\text{C}$  SPE-MAS NMR spectrum of KGMB-ac.

and the arbitrary scale can also be calibrated.  $^{13}\text{C}$  CP-MAS NMR spectra were recorded with different contact times (Fig. 4a and Fig. S14) to find a range over which the intensity ratio of the signals A and D, or E and D, did not vary significantly (here 5, 5.5 and 6 ms contact times). Therefore, for a semi-quantitative comparison on the same arbitrary scale the  $^{13}\text{C}$  CP-MAS spectra were recorded with an intermediate 5.5 ms contact time (Fig. 4b).

DA was quantified in all KGM samples from  $^{13}\text{C}$  CP-MAS spectra on the same arbitrary scale as the percentage of hexoses bearing an acetyl group using Eq. (1):

$$DA_{\text{CP}} = \frac{100 \cdot I_A}{I_D} \quad (1)$$

where  $I_A$  is the area of the signal A at 21 ppm from one methyl carbon of each acetyl group, and  $I_D$  is the area of the signal D at 103 ppm from one carbon (C-1) of each hexose. It was not practical to do enough replicates of the  $^{13}\text{C}$  CP-MAS measurement (each taking approximately a day) to assess the precision of  $DA_{\text{CP}}$  from them. The precision of the determined  $DA_{\text{CP}}$  was estimated through an empirical relation (Eq. (2)) established for determining degrees of branching in polyacrylates and polyolefins by solid-state  $^{13}\text{C}$  NMR (Castignolles, Graf, Parkinson, Wilhelm, & Gaborieau, 2009). In determining both DA and degree of branching, the ratio of two signal intensities was used, with that of the signal of limited sensitivity on the numerator. This relation is:

$$RSD = \frac{238}{\text{SNR}^{1.28}} \quad (2)$$

where RSD is the relative standard deviation of the determined intensity ratio, and SNR the signal-to-noise ratio of the signal with limited sensitivity on the numerator (signal A here). The methyl signal A was

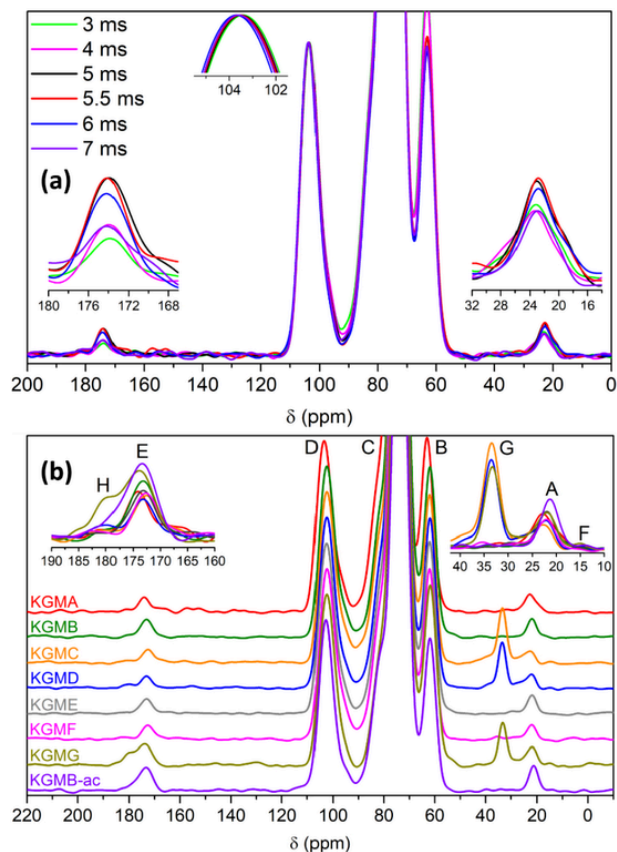


**Fig. 4.** Solid-state  $^{13}\text{C}$  CP-MAS NMR spectra (normalized to signal D at 103 ppm) of (a) KGMA with different contact times  $T_{\text{CP}}$  of 3, 4, 5, 5.5, 6, and 7 ms and (b) all KGM samples with  $T_{\text{CP}}$  of 5.5 ms.

chosen over the carbonyl signal E since the carbonyl signal H at 182 ppm of the excipient magnesium stearate strongly overlapped with signal E in KGMC, KGMD and KGMG (see Fig. 4b for signal labels and Table S6 for signal). In these samples, another magnesium stearate signal (G at 33 ppm) slightly overlapped with signal A. The relative signal intensities confirmed the qualitative purity assessment from FTIR spectroscopy that KGMG contained relatively more magnesium stearate than KGMC or KGME. The signal D at 103 ppm was not fully resolved from the signal C at 76 ppm for all KGM samples (Fig. 4b). However, for accurate quantification, full resolution (baseline resolution) of the signals of interest is needed. The resolution  $R_s$  of signals A and D, from signals G and C, respectively, was estimated with Eq. (3), typically used in chromatography:

$$R_s = \frac{\delta_1 + \delta_2}{\frac{1}{2} (fwhm_1 + fwhm_2)} \quad (3)$$

where  $\delta_1$  and  $\delta_2$  are the chemical shifts of the signals of interest, and  $fwhm_1$  and  $fwhm_2$  are their full widths at half maximum. For Gaussian lineshapes, full resolution occurs for  $R_s$  higher than 2. The resolution of signal D (and C) was almost complete, above 3.8 for all KGM samples (Table S7), indicating a very limited impact of the resolution on  $DA_{\text{CP}}$  determination. The resolution of signal A (and G) was between 2.1 and 2.6 for KGMC, KGMD and KGMG (Table S7), and this may affect  $DA_{\text{CP}}$  quantification when magnesium stearate is present. The  $DA_{\text{CP}}$  values of KGM samples (except KGM-B-ac) were between 4.4 and 7.9 a.u. (arbitrary units), and the acetylation reaction increased KGM-B's DA by 25 to 50% (Table S8).

### 3.3.3. Quantitative $^{13}\text{C}$ SPE-MAS

Following a published approach to calibrate the arbitrary scale (Gaborieau et al., 2010), quantitative  $^{13}\text{C}$  SPE-MAS spectra were recorded with sufficiently long delays between scans to ensure full relaxation.  $^{13}\text{C}$  longitudinal relaxation times ( $T_1$ ) of signals A and D were between 5 and 20 s in KGMB-ac, while the experiment was inconclusive for signal E (Fig. S15). Quantitative  $^{13}\text{C}$  SPE-MAS spectra of KGMA, KGMB, KGMB-ac and KGME were thus recorded using a relaxation delay of 100 s (Fig. 5; these spectra are quantitative for all signals except possibly the carbonyl signal E at 173 ppm). These samples were selected as they do not contain magnesium stearate, which potentially affects DA assessment. For good DA precision, measuring time was set to ensure a sufficient SNR (higher than 4), keeping in mind that SNR only increases with the square root of the measuring time. Eqs. (2) and (3)

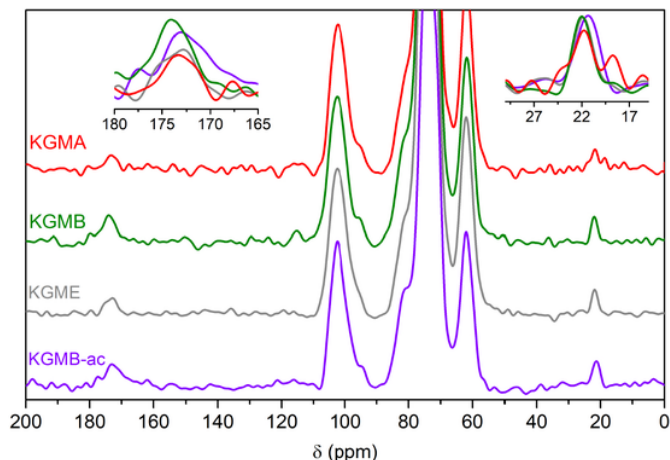


Fig. 5.  $^{13}\text{C}$  SPE-MAS spectra of selected KGM samples (quantitative for all signals except possibly the carbonyl signal at 173 ppm, normalized to signal D at 103 ppm).

were used to determine the quantitative  $DA_{\text{SPE}}$  values for KGMA, KGMB, KGMB-ac and KGME and their  $RSD$  from the  $^{13}\text{C}$  SPE-MAS spectra (Table S8). The quantitative  $DA_{\text{SPE}}$  values ranged from 4.8 to 7.4% of the hexoses for the KGM samples (except KGMB-ac), and the acetylation reaction on KGMB increased its quantitative  $DA_{\text{SPE}}$  value by 33 to 115%.

### 3.4. Comparison of solid-state spectroscopy methods

To assess the potential calibration of  $DA_{\text{CP}}$  and  $DA_{\text{IR}}$ , their relationship with the quantitative  $DA_{\text{SPE,q}}$  values was examined.  $DA_{\text{SPE,q}}$  against  $DA_{\text{CP}}$  exhibited a fair linear fit (Fig. 6a), with a  $R^2$  value of 0.6 reflecting the relatively large error bars of  $DA_{\text{SPE,q}}$  values. This fair fit indicated that the  $DA_{\text{CP}}$  values were, as expected, on an arbitrary scale, which can be calibrated through a correction factor. The slope of the linear fit of  $DA_{\text{SPE,q}}$  against  $DA_{\text{CP}}$  was thus used as a correcting factor for the  $DA_{\text{CP}}$  values using Eq. (4). This calibrates the  $DA_{\text{CP}}$  values by converting them to the same scale as the quantitative  $^{13}\text{C}$  SPE-MAS measurements. Furthermore, the  $RSD$  of the resulting quantitative  $DA_{\text{CP,q}}$  values was calculated with Eq. (5), determined from error calculations taking into account the errors on  $DA_{\text{CP}}$  and on the correcting factor (slope). The corrected values are given in Table S8 for all samples.

$$DA_{\text{CP,q}} = DA_{\text{CP}} \cdot (0.936 \pm 0.063) \quad (4)$$

$$RSD_{DA_{\text{CP,q}}} = DA_{\text{CP}} \cdot \sqrt{\left(\frac{RSD_{DA_{\text{CP}}}}{DA_{\text{CP}}}\right)^2 + \left(\frac{0.063}{0.936}\right)^2} \quad (5)$$

$DA_{\text{SPE,q}}$  against  $DA_{\text{IR}}$  exhibited no linear fit (Fig. 6b), as indicated by a negative  $R^2$  value. Thus, the  $DA_{\text{IR}}$  values could not be corrected through a simple correction factor.

For DA values determined by  $^{13}\text{C}$  NMR,  $DA_{\text{CP}}$  values (determined by semi-quantitative CP-MAS) were more precise (as shown by their smaller  $RSD$ s), while  $DA_{\text{SPE,q}}$  values (determined by quantitative SPE-MAS) were more accurate (Gaborieau et al., 2010). The corrected

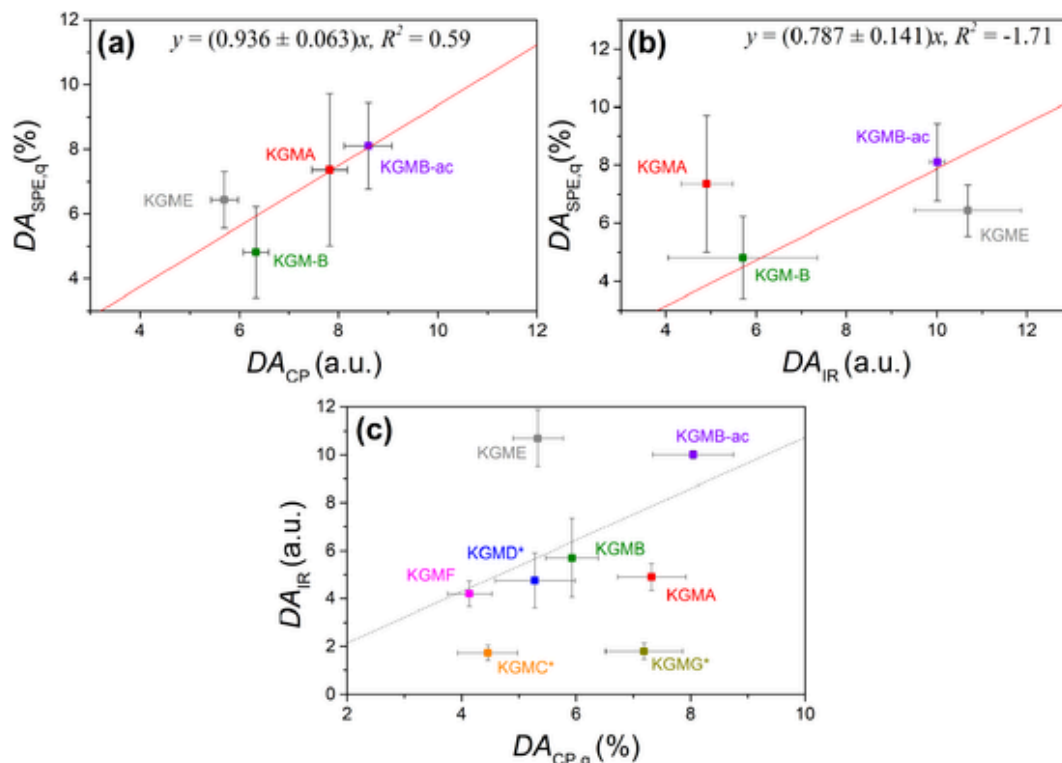


Fig. 6. DA values of KGM samples determined from different methods. (a)  $DA_{\text{SPE,q}}$  against  $DA_{\text{CP}}$ , (b)  $DA_{\text{SPE,q}}$  against  $DA_{\text{IR}}$ , with their linear fits (solid lines). (c)  $DA_{\text{IR}}$  against  $DA_{\text{CP,q}}$  with impure samples labelled with an \*, and the linear fit of the pure samples data shown as a guide to the eye (dotted line, see Fig. S20 for the fit).

$DA_{CP,q}$  values combined accuracy and better precision, and were the NMR-determined values selected for the comparison with FTIR-determined values. The  $DA_{IR}$  values were plotted against the  $DA_{CP,q}$  values for comparison (Fig. 6c), with the line of best fit of the pure samples shown.  $DA_{CP,q}$  values showed that acetylation ranged from 4 to 8% of hexoses in all samples (except KGMB-ac), in broad agreement with published studies (Alonso-Sande et al., 2009; Chua et al., 2012; Williams et al., 2000).  $DA_{CP,q}$  values also showed that the acetylation reaction on KGMB increased its  $DA$  by 15 to 60%. KGMA, KGME and KGMB-ac were significantly more acetylated than the other samples. KGMB was significantly more acetylated than KGMC and KGME.

$DA_{IR}$  values did not follow the same trend as  $DA_{CP,q}$  values (Fig. 6c), with strong deviations for KGME, KGMC and KGME. Excipients (including magnesium stearate) did not explain these deviations, as KGME does not contain excipients and did not follow the trend. The deviations may be explained by the limited penetration depth of the infrared irradiation (about 2  $\mu\text{m}$  (Sevenou et al., 2002)). ATR-FTIR thus yielded a biased measurement of  $DA$ , as only the outer layer of the KGM particles was measured. This allowed a qualitative assessment of the homogeneity of acetylation throughout the particles. Comparatively higher  $DA_{IR}$  values for KGME and KGMB-ac indicated higher acetylation in the outer layers of the particles than in their central parts. This is consistent with acetylating KGMB into KGMB-ac in a solvent that does not fully dissolve the KGM particles and leads to preferential acetylation in the outer layers of the particles. On the other hand, comparatively lower  $DA_{IR}$  values for KGMA, KGMC and KGME indicate lower acetylation in the outer layers of the particles than in their central parts. In an earlier study, acetylation was measured in the same product KGMA (named NKF) with an established titrimetric method and was found to be 2% w/w of acetyl-substituted residues in the KGM backbone (Chua et al., 2012), which corresponds to a  $DA$  of 8.1% of the hexoses (Gao & Nishinari, 2004); this is in broad agreement with the  $DA_{CP,q}$  value, but not the  $DA_{IR}$  value, determined in the present work.

#### 4. Conclusions

Common aqueous and organic solvents did not allow complete molecular solubility of selected KGM samples, yielding at best fine dispersions. A meaningful characterization of whole KGM samples in solution is not possible until KGM forms a true solution. Other avenues should be explored to fully dissolve KGM, with ionic liquids as potential alternative solvents already used for starch or cellulose and tested for glucomannans (El Seoud et al., 2007). Transparency is necessary but not sufficient for complete molecular solubility, and KGM's molecular solubility in transparent dispersions should be quantified, for example with solution-state NMR as done previously for starch (Schmitz et al., 2009) or poly(acrylic acid) (Maniego et al., 2017). Obtaining a true solution would open the way to the homogeneous chemical functionalization of KGM, and to the characterization of its molecular structure, for example of its sizes with size-exclusion chromatography, of its average composition by solution-state NMR, chromatography or capillary electrophoresis, or of their heterogeneity at the molecular level by separation techniques (e.g., chromatography, capillary electrophoresis) (Thevarajah et al., 2016b).

The critical assessment of different methods for KGM dissolution and for  $DA$  determination leads us to recommend the use of solid-state methods for  $DA$  determination to avoid bias due to incomplete dissolution. Solid-state spectroscopic methods were chosen and developed in this work to assess the degree of acetylation in KGM. Fast ATR-FTIR enabled a qualitative assessment of acetylation, which is selective to the outer layer of KGM particles, and identifying excipients like magnesium stearate. Thus, this method is recommended for qualitative (structure elucidation) but not quantitative ( $DA$  determination) sample analysis.

Solid-state  $^{13}\text{C}$  NMR allowed a meaningful quantification of the average degree of acetylation  $DA$  in KGM. Semi-quantitative measurements by  $^{13}\text{C}$  CP-MAS NMR allowed the comparison of samples on the same arbitrary scale; the precision of the measurement was assessed from the SNR of the methyl acetyl group. The calibration (with longer  $^{13}\text{C}$  SPE-MAS NMR measurements) of the arbitrary scale of the  $DA$  values from  $^{13}\text{C}$  CP-MAS provided quantitative  $DA$  values for selected KGM samples, ranging from 4 to 8% of the hexoses in the KGM backbone, in agreement with previously reported values. The present study provided the first meaningful quantification of  $DA$  in KGM in the solid state. It opens the way to the quantification of acetylation in a broader range of KGM samples. This analytical procedure can be applied to characterize the pharmaceutical grade of KGM and could be adopted by regulatory authorities as a pharmacopoeia standard. Most analyses of food-grade KGM currently depend on back-titration of glucose after complete hydrolysis of the given KGM powder (Chua et al., 2010). The proposed  $DA$  quantification methodology by solid-state NMR will provide better quality control of KGM, and support, for example, studies of the role of acetylation in functional properties like processing (e.g., gelation) of glucomannan and glucomannan acetate samples with a broader range of  $DA$  values, or KGM nutritional and health benefits.

#### CRediT authorship contribution statement

**Kash A. Bhullar:** Conceptualization, Methodology, Investigation, Formal analysis, Validation, Visualization, Writing – original draft, Writing – review & editing. **Michael I.M. Horgan:** Conceptualization, Investigation, Formal analysis, Visualization, Writing – original draft, Writing – review & editing. **Ashley Le:** Methodology, Investigation, Writing – review & editing. **David Fania:** Methodology, Investigation, Writing – review & editing. **Richard Wuhner:** Resources, Methodology, Formal analysis, Writing – review & editing. **Valentina Razmovski-Naumovski:** Conceptualization, Project administration, Resources, Supervision, Visualization, Writing – review & editing. **Kelvin Chan:** Conceptualization, Project administration, Resources, Supervision, Visualization, Writing – review & editing. **Patrice Castignolles:** Conceptualization, Formal analysis, Methodology, Project administration, Resources, Supervision, Visualization, Writing – original draft, Writing – review & editing. **Marianne Gaborieau:** Conceptualization, Investigation, Formal analysis, Methodology, Project administration, Resources, Supervision, Validation, Visualization, Writing – original draft, Writing – review & editing.

#### Declaration of competing interest

The authors declare that they have no known competing financial interests or personal relationships that could have appeared to influence the work reported in this paper.

#### Acknowledgments

The authors acknowledge the Advanced Materials Characterization Facility (AMCF) of Western Sydney University for access to instrumentation and help from staff, some suppliers for KGM research samples, Wayne Higginbotham and Paul Roddy for assistance in acetylation reactions. This research did not receive any specific grant from funding agencies in the public, commercial, or not-for-profit sectors.

#### Appendix A. Supplementary data

Supplementary data to this article can be found online at <https://doi.org/10.1016/j.carbpol.2022.119659>.

## References

- Alonso-Sande, M., Teijeiro-Osorio, D., Remunan-Lopez, C., & Alonso, M.J. (2009). Glucomannan, a promising polysaccharide for biopharmaceutical purposes. *European Journal of Pharmaceutics and Biopharmaceutics*, 72, 453–462.
- Brigden, C.J., & Wilkinson, S.G. (1985). Structural studies of acidic glucomannans from strains of *Serratia marcescens* O14 and O6. *Carbohydrate Polymers*, 138, 267–276.
- Castignolles, P., Graf, R., Parkinson, M., Wilhelm, M., & Gaborieau, M. (2009). Detection and quantification of branching in polyacrylates by size-exclusion chromatography (SEC) and melt-state <sup>13</sup>C NMR spectroscopy. *Polymer*, 50, 2373–2383.
- Chua, M., Baldwin, T.C., Hocking, T.J., & Chan, K. (2010). Traditional uses and potential health benefits of *Amorphophallus konjac* K. Koch ex n.E.Br. *Journal of Ethnopharmacology*, 128, 268–278.
- Chua, M., Chan, K., Hocking, T.J., Williams, P.A., Perry, C.J., & Baldwin, T.C. (2012). Methodologies for the extraction and analysis of konjac glucomannan from corms of *Amorphophallus konjac* K. Koch. *Carbohydrate Polymers*, 87, 2202–2210.
- Du, X., Li, J., Chen, J., & Li, B. (2012). Effect of degree of deacetylation on physicochemical and gelation properties of konjac glucomannan. *Food Research International*, 46, 270–278.
- El Seoud, O.A., Koschella, A., Fidale, L.C., Dorn, S., & Heinze, T. (2007). Applications of ionic liquids in carbohydrate chemistry: A window of opportunities. *Biomacromolecules*, 8, 2629–2647.
- Felix da Silva, D., Ogawa, C.Y.L., Sato, F., Neto, A.M., Larsen, F.H., & Matumoto-Pintro, P.T. (2020). Chemical and physical characterization of konjac glucomannan-based powders by FTIR and <sup>13</sup>C MAS NMR. *Powder Technology*, 361, 610–616.
- Furuhata, K.I., Koganei, K., Chang, H.S., Aoki, N., & Sakamoto, M. (1992). Dissolution of cellulose in lithium bromide organic-solvent systems and homogeneous bromination of cellulose with *N*-bromosuccinimide triphenylphosphine in lithium bromide *N,N*-dimethylacetamide. *Carbohydrate Research*, 230, 165–177.
- Gaborieau, M., & Castignolles, P. (2011). Size-exclusion chromatography (SEC) of branched polymers and polysaccharides. *Analytical and Bioanalytical Chemistry*, 399, 1413–1423.
- Gaborieau, M., Nebhani, L., Graf, R., Barner, L., & Barner-Kowollik, C. (2010). Accessing quantitative degrees of functionalization on solid substrates via solid-state NMR spectroscopy. *Macromolecules*, 43, 3868–3875.
- Gao, S.J., & Nishinari, K. (2004). Effect of degree of acetylation on gelation of konjac glucomannan. *Biomacromolecules*, 5, 175–185.
- Gidley, M.J., McArthur, A.J., & Underwood, D.R. (1991). <sup>13</sup>C NMR characterization of molecular structures in powders, hydrates and gels of galactomannans and glucomannans. *Food Hydrocolloids*, 5, 129–140.
- Gomes Neto, R.J., Genevro, G.M., Paulo, L.D.A., Lopes, P.S., de Moraes, M.A., & Beppu, M.M. (2019). Characterization and in vitro evaluation of chitosan/konjac glucomannan bilayer film as a wound dressing. *Carbohydrate Polymers*, 212, 59–66.
- Huang, L., Takahashi, R., Kobayashi, S., Kawase, T., & Nishinari, K. (2002). Gelation behavior of native and acetylated konjac glucomannan. *Biomacromolecules*, 3, 1296–1303.
- Kato, K., & Matsuda, K. (1969). Studies on the chemical structure of konjac mannan. *Agricultural and Biological Chemistry*, 33, 1446–1453.
- Katsuraya, K., Okuyama, K., Hatanaka, K., Oshima, R., Sato, T., & Matsuzaki, K. (2003). Constitution of konjac glucomannan: Chemical analysis and <sup>13</sup>C NMR spectroscopy. *Carbohydrate Polymers*, 53, 183–189.
- Keithley, J., & Swanson, B. (2005). Glucomannan and obesity: A critical review. *Alternative Therapies in Health and Medicine*, 11, 30.
- Kok, M.S., Abdelhameed, A.S., Ang, S., Morris, G.A., & Harding, S.E. (2009). A novel global hydrodynamic analysis of the molecular flexibility of the dietary fibre polysaccharide konjac glucomannan. *Food Hydrocolloids*, 23, 1910–1917.
- Koroskenyi, B., & McCarthy, S.P. (2001). Synthesis of acetylated konjac glucomannan and effect of degree of acetylation on water absorbency. *Biomacromolecules*, 2, 824–826.
- Kruk, J., Kaczmarczyk, K., Ptaszek, A., Goik, U., & Ptaszek, P. (2017). The effect of temperature on the colligative properties of food-grade konjac gum in water solutions. *Carbohydrate Polymers*, 174, 456–463.
- Maniego, A.R., Sutton, A.T., Gaborieau, M., & Castignolles, P. (2017). Assessment of the branching quantification in poly(acrylic acid): Is it as easy as it seems? *Macromolecules*, 50, 9032–9041.
- Morcombe, C.R., & Zilm, K.W. (2003). Chemical shift referencing in MAS solid state NMR. *Journal of Magnetic Resonance*, 162, 479–486.
- Nishinari, K. (2000). Konjac glucomannan. *Developments in Food Science*, 41, 309–330.
- Nishinari, K., Williams, P., & Phillips, G. (1992). Review of the physico-chemical characteristics and properties of konjac mannan. *Food Hydrocolloids*, 6, 199–222.
- Ratcliffe, I., Williams, P.A., Viebke, C., & Meadows, J. (2005). Physicochemical characterization of konjac glucomannan. *Biomacromolecules*, 6, 1977–1986.
- Rebierre, J., Heuls, M., Castignolles, P., Gaborieau, M., Rouilly, A., Violleau, F., & Durrieu, V. (2016). Structural modifications of cellulose samples after dissolution into various solvent systems. *Analytical and Bioanalytical Chemistry*, 408, 8403–8414.
- Rinaudo, M. (2006). Characterization and properties of some polysaccharides used as biomaterials. *Macromolecular Bioscience*, 245–246, 549–557.
- Schmitz, S., Dona, A.C., Castignolles, P., Gilbert, R.G., & Gaborieau, M. (2009). Assessment of the extent of starch dissolution in dimethyl sulfoxide by <sup>1</sup>H NMR spectroscopy. *Macromolecular Bioscience*, 9, 506–514.
- Sevenou, O., Hill, S.E., Farhat, I.A., & Mitchell, J.R. (2002). Organisation of the external region of the starch granule as determined by infrared spectroscopy. *International Journal of Biological Macromolecules*, 31, 79–85.
- Singh, S., Singh, G., & Arya, S.K. (2018). Mannans: An overview of properties and application in food products. *International Journal of Biological Macromolecules*, 119, 79–95.
- Spies, H.W. (2017). 50th anniversary perspective: The importance of NMR spectroscopy to macromolecular science. *Macromolecules*, 50, 1761–1777.
- Stephen, A.M., & Churms, S.C. (2006). Introduction. In A.M., Stephen, G.O., Phillips, & P.A., Williams (Eds.), *Food polysaccharides and their applications* (pp. 1–24). Boca Raton: CRC Taylor & Francis.
- Thevarajah, J.J., Bulanadi, J.C., Wagner, M., Gaborieau, M., & Castignolles, P. (2016a). Towards a less biased dissolution of chitosan. *Analytica Chimica Acta*, 955, 258–268.
- Thevarajah, J.J., Sutton, A.T., Maniego, A.R., Whitty, E.G., Harrison, S., Cottet, H., ... Gaborieau, M. (2016b). Quantifying the heterogeneity of chemical structures in complex charged polymers through the dispersity of their distributions of electrophoretic mobilities of compositions. *Analytical Chemistry*, 88, 1674–1681.
- Vieira, M., & Gil, A. (2005). A solid state NMR study of locust bean gum galactomannan and konjac glucomannan gels. *Carbohydrate Polymers*, 60, 439–448.
- Williams, M.A.K., Foster, T.J., Martin, D.R., Norton, I.T., Yoshimura, M., & Nishinari, K. (2000). A molecular description of the gelation mechanism of konjac mannan. *Biomacromolecules*, 1, 440–450.
- Wu, C., Peng, S., Wen, C., Wang, X., Fan, L., Deng, R., & Pang, J. (2012). Structural characterization and properties of konjac glucomannan/curdilan blend films. *Carbohydrate Polymers*, 89, 497–503.
- Yang, G., Xiong, X.P., & Zhang, L. (2002). Microporous formation of blend membranes from cellulose/konjac glucomannan in NaOH/thiourea aqueous solution. *Journal of Membrane Science*, 201, 161–173.
- Zhang, Y.-Q., Xie, B.-J., & Gan, X. (2005). Advance in the applications of konjac glucomannan and its derivatives. *Carbohydrate Polymers*, 60, 27–31.
- Zhu, F. (2018). Modifications of konjac glucomannan for diverse applications. *Food Chemistry*, 256, 419–426.